

Real-space composition–depth profiling in polymeric samples to 3 nm resolution using the ${}^2\text{H}({}^3\text{He}, {}^1\text{H}){}^4\text{He}$ nuclear reaction

T. Kerle⁺, F. Scheffold⁺, A. Losch⁺, U. Steiner⁺, G. Schatz⁺⁺ and J. Klein^{**}

⁺ Department of Materials and Interfaces, Weizmann Institute of Science, 76100 Rehovot, Israel

^{**} Fakultät für Physik, Universität Konstanz, D-78434 Konstanz, FRG

Direct depth profiling techniques to date have largely lacked the necessary depth resolution to investigate interfacial phenomena of the order of the bulk correlation length (5–10 nm for a wide range of systems). Here we investigate the optimal spatial resolution and depth of probe that may be attained for composition – depth profiling of polymeric samples via nuclear reaction analysis (NRA) using the ${}^2\text{H}({}^3\text{He}, {}^1\text{H}){}^4\text{He}$ reaction. We find that the spatial resolution can be greatly improved by using a grazing incidence geometry of the incident ${}^3\text{He}$ beam on the sample, and analyzing the emitted protons in a backwards direction. This results in spatial resolutions down to about 3 nm at the sample surface, compared to a value of some 7 nm or more previously reported in earlier studies when emitted α -particles were detected in the forward direction. At the same time the depth to which samples can be profiled via the backwards emitted protons may be considerably extended relative to the α -particle detection mode, when the ${}^3\text{He}$ beam impinges on the sample surface at normal incidence (up to about 4 μm into the sample for incident energies of 1.2 MeV in the proton-detection mode compared to only 1 μm for the equivalent α -particle detection mode).

1. Introduction

An important spatial scale at polymer surfaces and at interfaces between different polymers is frequently the bulk correlation length [1], which is often around 5–10 nm for a wide range of conditions and materials. For studies of near-surface effects in polymers, which hold a considerable scientific as well as technological interest, the most commonly used direct depth profiling techniques largely lack, or are on the verge of, the necessary depth resolution to discriminate structure on this scale. In comparison to indirect methods such as X-ray and neutron reflectometry, the advantages of direct profiling methods are clear: the results are model independent and the data analysis is simplified significantly. Among the more widely used direct space methods, the highest spatial resolutions have been achieved by dynamic secondary-ion mass spectroscopy (SIMS) and low-energy forward recoil scattering (LE-FRES) [2]. These have typical spatial resolutions (Gaussian half-widths) at the sample surfaces of $\sigma = 5$ nm (SIMS) [3] and $\sigma = 7$ nm (LE-FRES) [4]. Another high resolution method, widely used in our laboratory [5–11] and by other groups [12–15], is non-resonant nuclear reaction analysis (NRA). In this paper we describe the extension of this technique to spatial resolutions higher than any so far achieved with these common profiling approaches [3–5], and which enable the probing of polymer surfaces at sub-correlation-length scales.

The basic idea is simply described by reference to the nuclear reaction ${}^2\text{H}({}^3\text{He}, {}^1\text{H}){}^4\text{He}$, which has been extensively used for depth profiling in polymers in recent years [5, 7, 8, 10, 11]. A beam of energetic charged ${}^3\text{He}$ particles is incident on a sample, some of whose molecules are labeled with deuterium (deuterium labeling of polymers is readily achieved and is chemically innocuous), and as they penetrate it the reaction takes place at different depths; protons (${}^1\text{H}$) and α -particles (${}^4\text{He}$) are emitted as the reac-

tion products, and are detected by a suitably placed detector. The energy of these detected particles is a function of the depth z at which the reaction occurred, while their abundance at this energy gives a measure of the concentration ϕ of ${}^2\text{H}$ -labeled molecules at that depth. Hence a composition–depth profile $\phi(z)$ may be generated. The cross-section and the angular distribution of the protons of the ${}^2\text{H}({}^3\text{He}, {}^1\text{H}){}^4\text{He}$ nuclear reaction were measured as early as 1955 by Kunz [16] and recently remeasured by Möller and Besenbacher [17]. The first use of this reaction for depth profiling was reported by Pronko and Pronko in 1973 [18] and later on Dieumegard et al. [19] pointed out the advantages of proton detection. Chaturvedi et al. and Payne et al. were the first to apply the ${}^2\text{H}({}^3\text{He}, {}^1\text{H}){}^4\text{He}$ NRA for depth profiling polymer samples [6, 12]. While Chaturvedi detected the outgoing α -particles, Payne made use of the emerging protons. The resolutions achieved at the surface of the samples were $\sigma = 7$ nm in the case of the alpha detection and $\sigma = 18$ nm for the protons. The focus of the present work was to investigate conditions for which the depth resolution and range of the ${}^2\text{H}({}^3\text{He}, {}^1\text{H}){}^4\text{He}$ NRA could be optimized. Earlier work using this reaction involved composition–depth profiling using mainly the ${}^4\text{He}$ (α -particle) detection mode [8]; in this paper we treat primarily the ${}^1\text{H}$ (proton) detection mode.

2. Experimental

2.1. Materials and sample preparation

The samples used in this study consisted of a layer of fully deuterated polystyrene (dPS) mounted on a wafer of optically polished silicon. The monodisperse ($M_w/M_n < 1.04$) polystyrene had a molecular weight of 1×10^6 g mol⁻¹ and was obtained from Polymer Laboratories Ltd. (Church Stretton, UK). The silicon wafers were purchased either from Aurel GmbH, Germany, or Institute of Electronic Materials Technology, Warsaw, Poland. The polymer films were prepared by spin casting a toluene solution of

Fax: +972-8-344138

e-mail: bpklein@weizmann.weizmann.ac.il

dPS on the silicon wafers (1 cm × 2 cm). The thickness of the films was controlled by either the concentration of the solutions, or the rotational frequency of the spin caster.

2.2. Method

Figure 1 shows the experimental configuration for NRA in the α -particle detection mode (α -NRA, Fig. 1 a), and in the proton-detecting mode (proton NRA, Fig. 1 b). A collimated beam of monoenergetic ^3He ions from the 3MV Van de Graaff accelerator at the Weizmann Institute is incident on a sample containing a mixture of a deuterated and hydrogenated polymer. The energy of the ^3He particles typically has a value $E_{^3\text{He}}$ in the range of 0.7 to 1.2 MeV, with an energy spread of ± 10 keV.

The probability of the incoming ^3He ions reacting with the ^2H atoms labeling the dPS chains in the sample

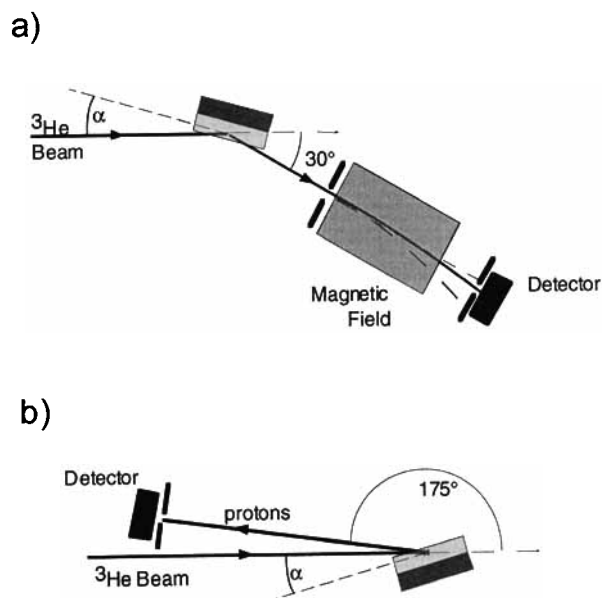


Fig. 1. Schematic illustration of the experimental configuration for NRA based on the $^2\text{H}(^3\text{He}, ^1\text{H})^4\text{He}$ reaction: detection of (a) forwards-emitted ($\psi = 30^\circ$) ^4He (α -NRA) and (b) backwards-emitted ($\psi = 175^\circ$) ^1H (proton-NRA).

depends on the reaction cross-section (with a maximum value of 900 mbarn at $E_{^3\text{He}} = 650$ keV [17]). The exothermic reaction $^3\text{He} + ^2\text{H} \rightarrow ^1\text{H} + ^4\text{He} + Q$ has a Q value of 18.352 MeV in the center of mass frame. The energy of the reaction products in the laboratory frame is determined by the reaction kinematics [20], which are a function of the energy of the incident ^3He ion $E_{^3\text{He}}$ at the point of the reaction, and of the scattering angle. The ^3He particles penetrating the polymer sample lose energy due to inelastic electronic scattering processes inside the sample – nuclear scattering is not relevant, since the cross-section for nuclear stopping processes is in our case roughly three orders of magnitude less than the one for electronic stopping [20]. The reaction products also lose energy due to

electronic scattering processes before emerging from the sample and reaching the detector. Hence the depth at which the reaction occurs can be identified uniquely by the energy of the detected α -particles and protons. Due to statistical fluctuations in the number of scattering processes, energy straggling occurs both for the incident ^3He particles prior to the reaction and for the emerging particles before they leave the sample on their way to the detector. This results in a broadening of energies of the emerging particles with increasing depth of reaction, resulting in decreasing depth resolution. In the case of the α -NRA a magnet is used to deflect the unwanted elastically scattered ions, as described earlier [6]. The protons are detected by a high resolution surface barrier detector, Ortec model BA-014-025-1500, with a proton energy resolution of 9 keV (FWHM).

The energy spectra thus obtained (number of particles vs. their energy) need to be converted into deuterium concentration versus depth profiles. Using semiempirical formulas for the stopping power given by Ziegler [21–24] to calculate the energy–depth relation, and taking account of the cross-section at different energies (i.e. different depths), we can readily convert the spectra into concentration–depth profiles of the deuterium (and hence of the deuterated polymer fraction) inside the specimen [25, 26].

To obtain the system resolution σ we measured profiles of polystyrene films of different thicknesses mounted on silicon wafers. The profile of a single film of constant deuterium concentration would resemble a “top hat” function for a detection system with perfect resolution. The actual depth profile of such a film is a convolution of this shape with a Gaussian of root mean square deviation $\sigma(z)$ representing the finite system resolution:

$$\phi(z) = \frac{1}{\sqrt{2\pi}} \int_{-\infty}^{\infty} \frac{1}{\sigma(\xi)} (\theta(z - z_1) - \theta(z - z_2)) e^{-(\xi - z)^2 / 2\sigma(\xi)^2} d\xi \quad (1)$$

$\phi(z)$ is the volume fraction of the deuterated polymer at depth z , $\theta(z)$ are step functions at depth z , and z_1 and z_2 the positions of the air/polymer and polymer/silicon interfaces. $\sigma(z)$ is the depth(z)-dependent gaussian half-width of the resolution function at depth z . Since σ can be assumed constant around z_1 or z_2 , each convoluted step is given by an error function. The error function can be very well approximated by a hyperbolic tangent, given by

$$\phi(z) = \frac{1}{2} + \frac{1}{2} \tanh\left(\frac{z - z_i}{w}\right) \quad i = 1, 2 \quad (2)$$

where $w = \sigma\sqrt{12}/\pi$ ($\approx 1.1\sigma$) is a direct measure of the system resolution. The error made by making this approximation is negligible in comparison with the scatter in the data points [9].

Figure 2 shows a typical depth profile of a uniform deuterated polymer film obtained by proton NRA. The energy of the incoming ^3He beam was 700 keV and the angle α between beam and sample (Fig. 1 b) was 8° . The solid curve is a best (least squares) fit using the hyperbolic tangent expression (2) at each interface. The corresponding

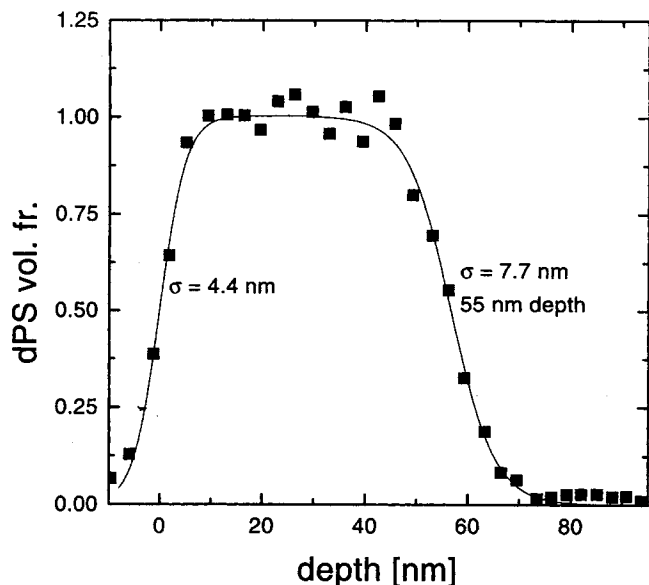


Fig. 2. Typical composition–depth profile of a uniform deuterated polymer film obtained by proton NRA. The energy of the incoming ${}^3\text{He}$ beam is $E_{3\text{He}} = 700$ keV and the angle between beam and sample is $\alpha = 8^\circ$. The solid curve is the least mean squares fit with the hyperbolic tangent expression of Eq. (2) to both interfaces, where $\sigma = 4.4$ nm at the air/polymer surface and $\sigma = 7.7$ nm at a depth of 55 nm (where the polymer/silicon interface is located) are the best fit values of the resolution.

resolutions are $\sigma = 4.4$ nm at the air/polymer surface and $\sigma = 7.7$ nm at a depth $z = 55$ nm, where the polymer/silicon interface is located. In this way values of the resolution σ are generated for different depths, scattering angles, incident energies $E_{3\text{He}}$ and incident angles α .

3. Results and discussion

Depth resolution is governed by a number of parameters. It is convenient to differentiate between effects that influence the resolution at the surface, those that influence it in the bulk of the sample, and other effects.

Bulk effects include the electronic losses noted earlier, so that incoming ${}^3\text{He}$ ions will have different energies E_{in} at different depths in the sample where the reaction takes place. These differences are amplified by the reaction kinematics [16, 17]: the amplification factor $F(E_{\text{in}}, \psi)$ is defined as $F(E_{\text{in}}, \psi) = \partial E_{\text{out}}(E_{\text{in}}, \psi) / \partial E_{\text{in}}$, where E_{out} is the energy of an outgoing particle (proton or α -particle) and ψ is the scattering angle. Clearly the larger the absolute value of F the better the resolution [6]. For protons and for α -particles emitted in a forward direction F is positive and has a value around 2 (which varies with ψ and E_{in}). For particles emitted in a backward direction F drops to around 1 (and is negative – the lower the energy of the incoming particles, the higher the energy of the backwards-emitted protons and alphas): this clearly reduces the achievable resolution for the backwards-emitted protons. Unfortunately, forward-emitted protons in this reaction, while being associated with a higher amplification factor, also have much

higher E_{out} : $E_{\text{out}} \approx 17$ MeV for $E_{\text{in}} = 900$ keV for forward emission, compared with $E_{\text{out}} \approx 12$ MeV for backwards-emitted protons. This requires a detector with a much thicker depletion layer, and hence worse intrinsic energy resolution; and detection of forward-emitted protons was not employed in the present study. A clear advantage associated with proton as opposed to α -particle detection has to do with the much higher energies E_{out} of the former, even in a backwards direction: energy losses in traversing the sample are lower at higher energies, so that the energy straggling described earlier, which reduces depth resolution, is significantly lower for the protons on their way out of the sample.

Resolution at the surface does not suffer from straggling but is controlled by other factors: the incoming beam has a certain energy distribution (± 10 keV), which results again in an energy distribution of the reaction particles. Together with the limited energy resolution of the detector used this leads to a finite energy resolution at the sample surface. Depending on the incident angle of the incoming beam this energy resolution transforms into different depth resolutions – in general, the smaller the angle α between beam and sample (Fig. 1 b), the better the surface resolution, which can be understood by simple geometric considerations [6, 27].

This effect is seen clearly in Fig. 3 – the resolution of proton NRA at 1.2 MeV versus depth was determined for several different incident beam angles: data for 15° , 45° and 90° (normal incidence) are shown, while data for 30° and 60° (omitted for clarity) demonstrate intermediate values as expected. The dotted lines shown in this and in the following figure are intended as guides to the eye. With decreasing incident angle the surface resolution gets better – but at the same time the actual depth that can be usefully profiled gets smaller. It should be noted that in the case of 90° (normal) incidence, incident energies $E_{3\text{He}} = 1.2$ MeV in the proton NRA mode enable a resolution $\sigma \approx 150$ nm even at a probing depth of ca. $4 \mu\text{m}$, i.e. a spatial resolution which is some 4% of the total depth. At the other end of the spectrum, when aiming for the highest surface resolutions (but lower probing depths), the smallest incident angles α should not be chosen lower than 2° , as the accuracy of determining α (with our experimental setup) then becomes a limiting factor (in Fig. 5 we demonstrate the high resolution case of $\alpha = 4^\circ$). Focusing the beam to a beamspot of well-defined lateral size (< 2 mm) is also no longer possible at such small angles.

A more general advantage for proton as compared to α -particle detection has to do with the angular energy spread $S(E_{\text{in}}, \psi) = \partial E_{\text{out}}(E_{\text{in}}, \psi) / \partial \psi$ of the backwards-emitted (scattering angle $\psi = 175^\circ$) protons, which is some 10 times smaller than for forward emitted ($\psi = 30^\circ$) alphas. This implies that the counting rate can be greatly increased by opening the detector slit, with little corresponding loss of resolution. A useful corollary is that, due to this insensitivity to the scattering angle, this position of the polymer/air interface may be determined with a reproducibility of ± 1 nm between consecutive profiling runs. This enables depletion of the deuterated species at the sample surface to be detected, a possibility which has been used to examine

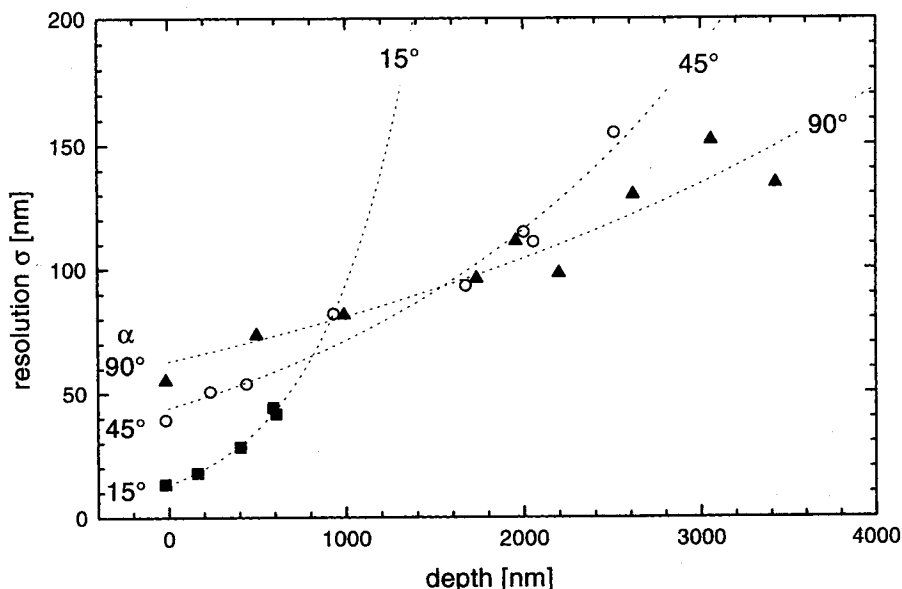


Fig. 3. Spatial resolution for backwards emitted ($\psi = 176^\circ$) proton NRA at $E_{3\text{He}} = 1.2$ MeV versus depth for different incident beam angles α : 15° (squares), 45° (circles) and 90° (triangles).

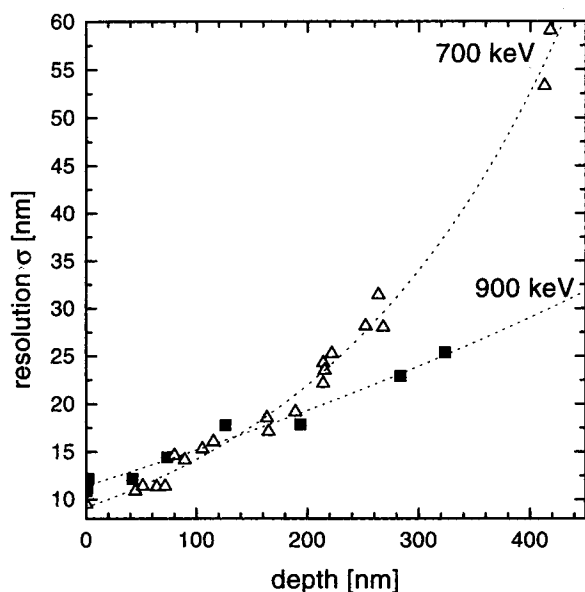


Fig. 4. Resolution of proton NRA at 700 keV (triangles) and 900 keV (squares) versus depth for an incident beam angle of 15° .

surface segregation of non-deuterated molecules to the surface of a deuterated/non-deuterated polymer mixture [10].

A further resolution improvement can be achieved by choosing a lower incoming energy for the ^3He ions. Since the stopping power increases with decreasing beam energy, the energy difference of an ion at the surface and an ion at a given depth z is bigger for lower incoming energies. There is a corresponding increase in the energy difference for outgoing particles from reactions at the surface and from reactions at the depth z . This increase acts to improve the depth resolution. Figure 4 shows a comparison between the resolution versus depth curves for different incoming ^3He energies, $E_{3\text{He}} = 700$ keV and 900 keV. The scattering geometry was the same in both cases: inci-

dent angle $\alpha = 8^\circ$ and detection of the backwards-emitted protons at an angle of 176° . Clearly the surface resolution is better for the lower incoming energy. At greater depths the resolutions “cross over” – the energy of the 700 keV incident beam drops to such low levels that the energy spread due to straggling, together with the low cross-section, become the dominant factors in reducing the resolution. For the same reason (for any given angle of incidence) the probing depth also decreases with decreasing $E_{3\text{He}}$. In principle it should also be possible to work with incoming energies even lower than 700 keV to improve the resolution at the surface. Our calculations indicate that the resolution achieved at $E_{3\text{He}} = 400$ keV would be 1.5 times better than at 700 keV, i.e. $\sigma \approx 2$ nm could be attained for $\alpha = 4^\circ$ [28]. In this case however the cross-section of the $^2\text{H}(^3\text{He}, ^1\text{H})^4\text{He}$ reaction, which has its maximum at 650 keV, drops rapidly with depth and the resulting depth range is rather limited. In addition the lower cross-section implies low reaction probabilities and hence low counting statistics at the sample surface. This in turn implies much longer counting times to reach reasonable statistics, so that beam damage to the surface increases and the sample surface gets rougher, degrading the resolution again. (AFM [29] and optical phase interference microscopy reveal that the RMS roughness of as-cast polystyrene films is of order 10 \AA). With a high enough resolution at the sample surface the surface roughening due to the beam damage can actually be monitored. Figure 5 shows the depth profile of the surface-near region of a uniform polystyrene film after measuring times of 15 min and of 1 h, at an incident angle $\alpha = 4^\circ$. At this grazing angle the resolution improves to $\sigma = 3.0$ nm (after 15 min beam time), but after 1 h beam time the resolution at the surface drops to $\sigma = 3.9$ nm due to the roughening of the surface by the incoming ^3He beam [30].

In summary, there are several interrelated factors that affect the resolution and depth range when profiling deut-

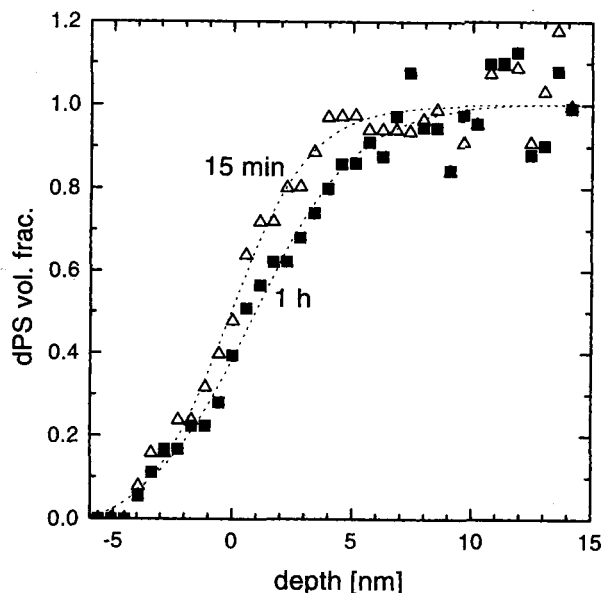


Fig. 5. Composition–depth profile of the near-surface region of a uniform polystyrene film after a measuring time of 15 min (triangles) and 1 h (squares), at incident angle $\alpha = 4^\circ$. Due to the roughening of the surface by the incoming ^3He beam for the longer measuring time, the resolution at the surface drops from $\sigma = 3.0$ nm (15 min) to $\sigma = 3.9$ nm (1 h).

erated molecules by detection of backwards-emitted protons from the $^2\text{H}(^3\text{He}, ^1\text{H})^4\text{He}$ reaction. Optimizing these factors we were able to achieve a depth resolution at the surface of a deuterated PS film of $\sigma = 3.0$ nm. This makes the $^2\text{H}(^3\text{He}, ^1\text{H})^4\text{He}$ NRA suitable for measuring surface structures that may not be resolvable with other direct depth profiling techniques, in particular where the length scale is of the order the bulk correlation length, 10 nm or less. Use has recently been made of this high resolution to investigate in detail the shape of a surface enrichment profile from a binary polymer mixture, and in particular to examine possible deviations in its shape from mean-field predictions [31].

4. Conclusions

We have examined the optimization of the $^2\text{H}(^3\text{He}, ^1\text{H})^4\text{He}$ nuclear reaction for composition–depth profiling of polymer samples. The depth resolution at the sample surface was improved by detecting protons at backward angles, using low energy ^3He beams and a grazing angle incident geometry. We were able to achieve spatial resolutions which, at values down to ~ 3 nm at the sample surface, are appreciably better than previously reported using this approach, and are comparable with or smaller than relevant correlation lengths in bulk polymeric samples.

References

[1] K. Binder, *Acta Polym.* **1995**, *46*, 204.
 [2] Other elegant if less common profiling techniques for thin polymer films include Rutherford backscattering off gold markers (see e.g. E.J. Kramer, P.F. Green, C.J. Palmstrom, *Polymer* **1984**, *25*, 473); and ^{15}N -nuclear reaction analysis (see e.g. K.-H. Giess-

ler, F. Rauch, M. Stamm, *Europhys. Lett.* **1994**, *27*, 605), for which a surface resolution of some 2 nm Gaussian half-width has been reported.
 [3] S.A. Schwarz, B.J. Wilkens, M.A.A. Pudensi, M.H. Rafailovich, J. Sokolov, X. Zhao, W. Zhao, X. Zheng, T. Russell, R.A.L. Jones, *Mol. Phys.* **1992**, *76*, 937.
 [4] J. Genzer, J.B. Rothmann, R.J. Composto, *Nucl. Instrum. Methods Phys. Res.* **1994**, *B 86*, 345.
 [5] U.K. Chaturvedi, U. Steiner, O. Zak, G. Krausch, J. Klein, *Phys. Rev. Lett.* **1989**, *63*, 616.
 [6] U.K. Chaturvedi, U. Steiner, O. Zak, G. Krausch, G. Schatz, J. Klein, *Appl. Phys. Lett.* **1990**, *56*, 1228.
 [7] J. Klein, *Science* **1990**, *250*, 640.
 [8] U. Steiner, J. Klein, L.J. Fetters, *Phys. Rev. Lett.* **1994**, *72*, 1498.
 [9] A. Losch, R. Salomonovic, U. Steiner, L.J. Fetters, J. Klein, *J. Polym. Sci., Polym. Phys.* **1995**, *33*, 1821.
 [10] F. Scheffold, A. Budkowski, U. Steiner, E. Eiser, J. Klein, L.J. Fetters, *J. Chem. Phys.* **1996**, *104*, 8795.
 [11] T. Kerle, J. Klein, K. Binder, *Phys. Rev. Lett.* **1996**, *77*, 1318.
 [12] R.S. Payne, A.S. Clough, P. Murphy, P.J. Mills, *Nucl. Instrum. Methods Phys. Res.* **1989**, *B 42*, 130.
 [13] G. Krausch, C.-A. Dai, E.J. Kramer, J.F. Marko, F. Bates, *Macromolecules* **1993**, *26*, 5566.
 [14] W. Straub, F. Bruder, R. Brenn, G. Krausch, H. Bielefeldt, A. Kirsch, O. Marti, J. Mlynek, J.F. Marko, *Europhys. Lett.* **1995**, *29*, 353.
 [15] M. Geoghegan, R.A.L. Jones, D.S. Sivia, J. Penfold, A.S. Clough, *Phys. Rev. E* **1996**, *53*, 825.
 [16] W.E. Kunz, *Phys. Rev.* **1955**, *97*, 456.
 [17] W. Möller, F. Besenbacher, *Nucl. Instrum. Methods Phys. Res.* **1980**, *168*, 111.
 [18] P.P. Pronko, J.G. Pronko, *Phys. Rev. B.* **1974**, *9*, 2870.
 [19] D. Dieumegard, Dubreuil, G. Amsel, *Nucl. Instrum. Methods Phys. Res.* **1979**, *166*, 431.
 [20] J.A. Davies, W.N. Lennard, I.V. Mitchell, in *Handbook of Modern Ion Beam Materials Analysis* (Eds: J.R. Tesmer, M. Nastasi), Materials Research Society, Pittsburgh, PA **1995**.
 [21] J.F. Ziegler, *Helium Stopping Powers and Ranges in All Elemental Matter*, Pergamon Press, New York **1977**.
 [22] J.F. Ziegler, *Handbook of Stopping Cross-Sections for Energetic Ions in All Elements*, Pergamon Press, New York **1980**.
 [23] J.F. Ziegler, J.P. Biersack, U. Littmark, *The Stopping and Range of Ions in Solids*, Pergamon Press, New York **1985**.
 [24] J.F. Ziegler, J.M. Manoyan, *Nucl. Instrum. Methods Phys. Res.* **1988**, *B 35*, 215.
 [25] An absolute calibration of the depth scales thus generated was recently carried out by comparing the NRA-generated thickness of uniform films of deuterated polymers with values of the thickness obtained from ellipsometry and X-ray reflectometry on the same samples. For PS the agreement between the three methods was within a few percent.
 [26] F. Zink, T. Kerle, M. Tarabia, D. Davidov, J. Klein, to be published.
 [27] In the ^4He detection mode too, reducing the angle α to 4° (as opposed to 15° used to date) and at the same time reducing the angle to the detector (to 10° – 15°) would likely result in some improvement to the resolution relative to the earlier-used configuration (Fig. 1a). The problem of greater scatter (for a given slit width) due to angular spread of the energies of the α -particles emitted in the forward direction would still remain, however.
 [28] Stable beam energies $E_{^3\text{He}} < 700$ keV are not at present feasible in our accelerator setup.
 [29] T. Kerle, R. Yerushalmi-Rozen, J. Klein, *Macromolecules*, in press.
 [30] This very slight reduction (< 1 nm) in the resolution is due to the extremely low grazing angle used. At the higher scattering angles used in earlier work, the effect of beam damage on the resolution are quite negligible, as demonstrated by the identity of profiles taken at different measuring times.
 [31] F. Zink, T. Kerle, J. Klein, *Macromolecules*, in press.

Received May 29, 1997

Final version September 8, 1997